Organic &
Biomolecular Chemistry

COMMUNICATION

Cite this: DOI: 10.1039/c9ob01828j

Received 19th August 2019,
Accepted 7th September 2019

DOI: 10.1039/c9ob01828j

rsc.li/obc

Synthesis of helical π-conjugated polymers bearing pyridine *N*-oxide pendants and asymmetric allylation of aldehydes in the helical cavity†

Tomoyuki Ikai *[a,b] and Takumu Yoshida[a]

Catalytically active chiral π-conjugated polymers (poly-1(NO)$_r$) bearing pyridine *N*-oxide pendants were synthesized by ternary copolymerization of a D-glucose-bound diethynyl compound with two types of thieno[3,4-*b*]thiophene comonomer, one of which contained a pyridine *N*-oxide group. When the pyridine *N*-oxide content in the copolymer was 10 mol% (poly-1(NO)$_{0.10}$), the polymer backbone formed a one-handed helical structure in acetonitrile. Pyridine *N*-oxide pendants arranged inside the helical cavity of poly-1(NO)$_{0.10}$ exhibited catalytic activity for the asymmetric allylation of benzaldehydes, producing the corresponding allyl alcohols with up to 43% ee.

Taking inspiration from exquisitely designed biomacromolecules containing helical geometries, such as DNA and proteins, various artificial helical polymers have been developed to date[1–7] and applied to chiral functional materials in various fields, such as chiral sensing,[8–11] chromatographic resolution[12–20] and circularly polarized luminescence.[21–27] The application of helical polymers to asymmetric catalysts has also attracted growing interest owing to the potential for characteristic catalytic activity, which is achieved through the one-handed helical arrangement of catalytically active units along the polymer backbone.[7] Thus far, various helical polymer-based asymmetric catalysts have been developed by embedding catalytically active pendants in artificial helices.[7,28–30] However, in most cases, catalytically active sites were located at the periphery of helical structures, with helical polymer-based asymmetric catalysis in the helical cavity achieved only in a few cases.[31,32]

Our group recently reported a series of chiral π-conjugated polymers, poly(arylene ethynylene)s, containing an optically active D-glucose-linked biphenyl (GLB) unit in the main chain.[26,33–35] Poly-**1** containing a thieno[3,4-*b*]thiophene (TT)-type comonomer unit is a representative example of these polymers (Fig. 1).[19,27] We also demonstrated that poly-**1** undergoes a reversible conformational transition between one-handed helix and random-coil structures in response to the exterior solvent environment, and that poly-**1** could be applied as a chiral stationary phase[19] and circularly polarized luminescent material.[27] Furthermore, when the poly-**1** main chain was folded into a helical conformation, the pendant groups on the TT repeating units were shown to be arranged inside the helical cavity (Fig. 1).

Considering the unique framework and chiral functions of GLB-based polymers, we anticipated that a novel helical polymer-based asymmetric catalyst, in which catalytically active units are arranged inside the helical cavity, could be developed through appropriate modification of the pendant groups in GLB-based polymers. In this study, novel GLB-based polymers (poly-**1**(NO)$_r$ in Scheme 1) bearing pyridine *N*-oxide groups as catalytically active sites on the TT units were designed and synthesized, and the helix-forming ability and asymmetric catalytic activity in the allylation of benzaldehydes were investigated (Fig. 2).

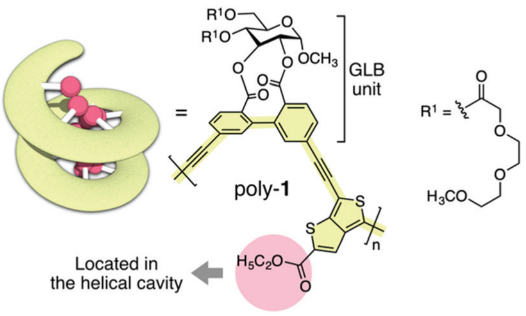

Fig. 1 Structure of poly-**1**.

---

[a] Graduate School of Natural Science and Technology, Kanazawa University, Kakuma-machi, Kanazawa 920-1192, Japan
[b] Department of Molecular and Macromolecular Chemistry, Graduate School of Engineering, Nagoya University, Chikusa-ku, Nagoya 464-8603, Japan. E-mail: ikai@chembio.nagoya-u.ac.jp

† Electronic supplementary information (ESI) available: Detailed experimental procedures, characterization of molecules/polymers and additional spectroscopic data. See DOI: 10.1039/c9ob01828j

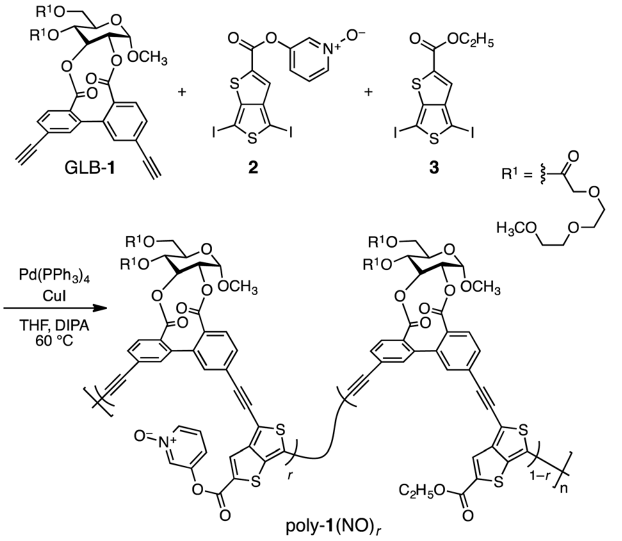

Scheme 1 Synthesis of GLB-based polymers bearing pyridine *N*-oxide groups (poly-**1**(NO)$_r$).

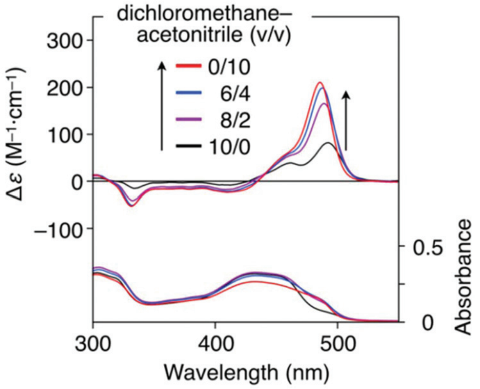

Fig. 3 CD and absorption spectra of poly-**1**(NO)$_{0.10}$ in dichloromethane–acetonitrile (10 : 0–0 : 10, v/v) at 0 °C, [glucose unit] = 1.0 × 10^{-4} M.

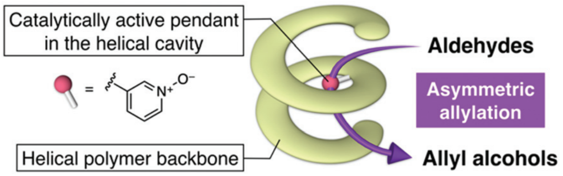

Fig. 2 Schematic illustration of helical polymer-based asymmetric catalysis occurring in the helical cavity.

A novel TT monomer bearing a catalytically active pyridine *N*-oxide group (**2**) was prepared from a commercially available phenol derivative and 4,6-diiodothieno[3,4-*b*]thiophene-2-carboxylic acid through a condensation reaction using activating agents (ESI Scheme S1†). The Sonogashira–Hagihara coupling copolymerization of GLB-**1** and **2** was first conducted using a palladium catalyst in a tetrahydrofuran (THF)–diisopropylamine mixture (5 : 1, v/v) at 60 °C, similar to our previously reported procedure.[19] However, as the resulting polymer showed very low solubility in common organic solvents, such as THF, chloroform and dichloromethane, further characterization could not be performed.

To ensure polymer solubility, the ternary copolymerization of GLB-**1**, **2** and **3** was performed as described above to afford poly-**1**(NO)$_r$, where *r* is the molar fraction of **2** in the monomer feed (Scheme 1). The ternary copolymerization performed with $[\text{GLB-}\mathbf{1}]_0/[\mathbf{2}]_0/[\mathbf{3}]_0 = 1.0:0.50:0.50$ still proceeded heterogeneously, affording a certain amount of an insoluble precipitate in the reaction system. When the feed mole fraction of **2** was decreased to 10% ($[\text{GLB-}\mathbf{1}]_0/[\mathbf{2}]_0/[\mathbf{3}]_0 = 1.0:0.10:0.90$), the copolymerization proceeded homogeneously, affording optically active poly-**1**(NO)$_{0.10}$ with a number-average molecular mass (M_n) of 1.3 × 10^4 g mol^{-1}, estimated by size-exclusion chromatography (SEC) (ESI Table S1†). The compositional ratio of the **2** and **3** units in the copolymer was confirmed to be almost identical to the feed ratios of these two TT comonomers by ^{1}H NMR and elemental analyses. The resulting poly-**1**(NO)$_{0.10}$ showed good solubility in organic solvents, such as THF, chloroform and dichloromethane, and was used in the subsequent study accordingly.

Absorption and circular dichroism (CD) spectra of poly-**1**(NO)$_{0.10}$ recorded in dichloromethane/acetonitrile (10 : 0–0 : 10, v/v) at 0 °C are shown in Fig. 3. In acetonitrile, poly-**1**(NO)$_{0.10}$ exhibited an intense CD signal in the absorption region of the π-conjugated backbone (400–520 nm), with the CD spectral patterns and intensities closely resembling those previously reported for poly-**1** in the helically folded state (ESI Fig. S1†).[19] This result indicated that poly-**1**(NO)$_{0.10}$ could form a one-handed helical conformation in acetonitrile. The spectral similarity between poly-**1**(NO)$_{0.10}$ and poly-**1** in acetonitrile also suggested that the pyridine *N*-oxide group introduced on the TT unit did not cause a noticeable change in the helical folding ability of GLB-based polymers. As observed for poly-**1**, the TT-bound ester pendants, including pyridine *N*-oxide units, were considered to be located inside the helical cavity. In contrast, when the chiroptical properties of poly-**1**(NO)$_{0.10}$ were measured in dichloromethane or dichloromethane/acetonitrile mixtures, its CD intensities significantly decreased with increasing dichloromethane content, accompanied by hyperchromic and hypsochromic shifts in the absorption spectra. Given the spectral pattern of poly-**1** with a random-coil conformation (ESI Fig. S1†),[19] the poly-**1**(NO)$_{0.10}$ backbone did not form a specific secondary structure in dichloromethane.

Poly-**1**(NO)$_{0.10}$ was then applied to an organocatalyst for the asymmetric addition of allyltrichlorosilane to benzaldehydes

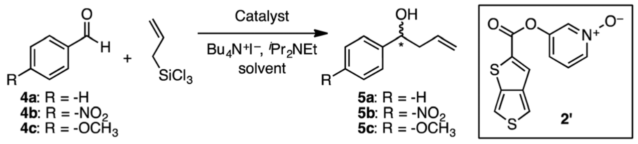

Scheme 2 Allylation reactions of benzaldehydes (**4**) with allyltrichlorosilane catalyzed by poly-**1**(NO)$_{0.10}$ and **2′**.

Table 1 Enantioselective allylation of benzaldehydes (**4**) with allyltrichlorosilane[a]

Entry	Catalyst	Temperature (°C)	Solvent	Substrate	Product	Yield (%)	ee[b] (%)
1	**2′**	0	Acetonitrile	**4a**	**5a**	25	—
2	Poly-**1**$(NO)_{0.10}$	0	Acetonitrile	**4a**	**5a**	25	26 (*R*)
3	Poly-**1**$(NO)_{0.10}$	−40	Acetonitrile	**4a**	**5a**	13	43 (*R*)
4	Poly-**1**$(NO)_{0.10}$	0	Dichloromethane	**4a**	**5a**	13	5 (*R*)
5	Poly-**1**$(NO)_{0.10}$	−40	Dichloromethane	**4a**	**5a**	8	6 (*R*)
6	Poly-**1**$(NO)_{0.10}$	−40	Acetonitrile	**4b**	**5b**	20	39 (*R*)
7	Poly-**1**$(NO)_{0.10}$	−40	Acetonitrile	**4c**	**5c**	15	31 (*R*)

[a] The reactions of **4** (0.5 M) with allyltrichlorosilane (1.2 equiv.) were carried out in the presence of a catalyst (1 mol%) and $^{i}Pr_2NEt$ (5.0 equiv.) in acetonitrile or dichloromethane. Reaction time = 48 h. [b] Determined by chiral HPLC. In parentheses are shown the absolute configuration of the major enantiomer assigned by the retention times and optical rotation signs reported in the literature [ref. 37].

(**4**) (Scheme 2).[36] Table 1 summarizes the results of allylation reactions of benzaldehydes using the poly-**1**$(NO)_{0.10}$-based organocatalyst. The corresponding result using the TT-based model compound (**2′**; see Scheme 2) as catalyst is shown for comparison. Poly-**1**$(NO)_{0.10}$ catalyzed the allylation reaction of **4a** in acetonitrile at 0 °C and gave the corresponding allyl alcohol (**5a**) in 25% yield after 48 h (entry 2), which was comparable to the result obtained using **2′** (25%, entry 1). This indicated that the pyridine *N*-oxide pendants in poly-**1**$(NO)_{0.10}$ caused little deterioration in the catalytic activity compared with that of **2′**, despite the catalytically active units in poly-**1**$(NO)_{0.10}$ being arranged in a closed environment inside the helical cavity. Importantly, poly-**1**$(NO)_{0.10}$ showed enantioselectivity in the asymmetric allylation reaction of **4a** in acetonitrile at 0 °C, affording (*R*)-**5a** with 26% enantiomeric excess (ee), as estimated by chiral HPLC (entry 2). When the reaction temperature was decreased to −40 °C (entry 3), the enantioselectivity improved to 43% ee. In contrast, when the allylation reactions were performed in dichloromethane at 0 and −40 °C in the presence of poly-**1**$(NO)_{0.10}$, the ee values of the product clearly decreased compared with the corresponding results in acetonitrile, while maintaining the absolute configuration of the major enantiomer (*R*-rich) (entries 4 and 5). These results indicated that the enantioselectivity obtained from the poly-**1**$(NO)_{0.10}$-based catalyst in acetonitrile was mainly attributed to the special arrangement of the catalytically active pendants inside the helical cavity. Poly-**1**$(NO)_{0.10}$ also showed moderate enantioselectivities in the allylation reactions using substituted benzaldehydes **4b** and **4c** as substrates, affording (*R*)-**5b** with 39% ee and (*R*)-**5c** with 31% ee, respectively (entries 6 and 7).

Conclusions

We have synthesized novel GLB-based polymers containing pyridine *N*-oxide groups as catalytically active pendants (poly-**1**$(NO)_r$) and investigated the solvent-induced helix-forming ability and asymmetric catalytic activity in the allylation of benzaldehydes with allyltrichlorosilane. Based on the chiroptical comparison of poly-**1**$(NO)_{0.10}$ with previously reported helically folded poly-**1**, the poly-**1**$(NO)_{0.10}$ backbone was concluded to form a one-handed helical conformation in acetonitrile, with TT-bound pyridine *N*-oxide pendants located inside the helical cavity. Furthermore, poly-**1**$(NO)_{0.10}$ was shown to function as a chiral organocatalyst in the asymmetric allylation of benzaldehydes, affording the corresponding allyl alcohols with up to 43% ee. We anticipate that more powerful GLB-based asymmetric organocatalysts with much higher catalytic activities and enantioselectivities can be developed through the delicate design of catalytically active pendant units. Related studies towards these goals are currently underway in our laboratory.

Conflicts of interest

There are no conflicts to declare.

Acknowledgements

This work was supported by the Japan Society for the Promotion of Science (JSPS) KAKENHI Grant No. 17K05875 (Grant-in-Aid for Scientific Research (C)) and 18H05209 (Grant-in-Aid for Specially Promoted Research). This work was also supported by the Shorai Foundation for Science and Technology.

Notes and references

1 M. M. Green, J.-W. Park, T. Sato, A. Teramoto, S. Lifson, R. L. B. Selinger and J. V. Selinger, *Angew. Chem., Int. Ed.*, 1999, **38**, 3138–3154.
2 T. Nakano and Y. Okamoto, *Chem. Rev.*, 2001, **101**, 4013–4038.
3 M. Suginome and Y. Ito, *Adv. Polym. Sci.*, 2004, **17**, 77–136.
4 M. Fujiki, *Chem. Rec.*, 2009, **9**, 271–298.
5 E. Yashima, K. Maeda, H. Iida, Y. Furusho and K. Nagai, *Chem. Rev.*, 2009, **109**, 6102–6211.
6 E. Schwartz, M. Koepf, H. J. Kitto, R. J. M. Nolte and A. E. Rowan, *Polym. Chem.*, 2011, **2**, 33–47.
7 E. Yashima, N. Ousaka, D. Taura, K. Shimomura, T. Ikai and K. Maeda, *Chem. Rev.*, 2016, **116**, 13752–13990.
8 E. Yashima, K. Maeda and T. Nishimura, *Chem. – Eur. J.*, 2004, **10**, 42–51.

9 E. Yashima and K. Maeda, *Macromolecules*, 2008, **41**, 3–12.

10 M. Fujiki, *Symmetry*, 2014, **6**, 677–703.

11 K. Maeda and E. Yashima, *Top. Curr. Chem.*, 2017, **375**, 72.

12 R. J. M. Nolte, A. J. M. Van Beijnen and W. Drenth, *J. Am. Chem. Soc.*, 1974, **96**, 5932–5933.

13 H. Yuki, Y. Okamoto and I. Okamoto, *J. Am. Chem. Soc.*, 1980, **102**, 6356–6358.

14 E. Yashima, S. Huang and Y. Okamoto, *J. Chem. Soc., Chem. Commun.*, 1994, 1811–1812.

15 C. Zhang, F. Liu, Y. Li, X. Shen, X. Xu, R. Sakai, T. Satoh, T. Kakuchi and Y. Okamoto, *J. Polym. Sci., Part A: Polym. Chem.*, 2013, **51**, 2271–2278.

16 K. Shimomura, T. Ikai, S. Kanoh, E. Yashima and K. Maeda, *Nat. Chem.*, 2014, **6**, 429–434.

17 K. Maeda, M. Maruta, K. Shimomura, T. Ikai and S. Kanoh, *Chem. Lett.*, 2016, **45**, 1063–1065.

18 J. Shen and Y. Okamoto, *Chem. Rev.*, 2016, **116**, 1094–1138.

19 T. Ikai, S. Awata, T. Kudo, R. Ishidate, K. Maeda and S. Kanoh, *Polym. Chem.*, 2017, **8**, 4190–4198.

20 D. Hirose, A. Isobe, E. Quiñoá, F. Freire and K. Maeda, *J. Am. Chem. Soc.*, 2019, **141**, 8592–8598.

21 S. Fukao and M. Fujiki, *Macromolecules*, 2009, **42**, 8062–8067.

22 K. Suda and K. Akagi, *Macromolecules*, 2011, **44**, 9473–9488.

23 D. Lee, Y.-J. Jin, H. Kim, N. Suzuki, M. Fujiki, T. Sakaguchi, S. K. Kim, W.-E. Lee and G. Kwak, *Macromolecules*, 2012, **45**, 5379–5386.

24 Y. Nagata, T. Nishikawa and M. Suginome, *Chem. Commun.*, 2014, **50**, 9951–9953.

25 K. Maeda, M. Maruta, Y. Sakai, T. Ikai and S. Kanoh, *Molecules*, 2016, **21**, 1487–1500.

26 T. Ikai, S. Shimizu, S. Awata, T. Kudo, T. Yamada, K. Maeda and S. Kanoh, *Polym. Chem.*, 2016, **7**, 7522–7529.

27 T. Ikai, S. Awata and K. Shinohara, *Polym. Chem.*, 2018, **9**, 1541–1546.

28 R. P. Megens and G. Roelfes, *Chem. – Eur. J.*, 2011, **17**, 8514–8523.

29 M. Suginome, T. Yamamoto, Y. Nagata, T. Yamada and Y. Akai, *Pure Appl. Chem.*, 2012, **84**, 1759–1769.

30 M. Suginome, T. Yamamoto and Y. Nagata, *J. Synth. Org. Chem., Jpn.*, 2015, **73**, 1141–1155.

31 N. Ousaka, T. Yamaguchi and E. Yashima, *Chem. Lett.*, 2014, **43**, 512–514.

32 M. Zurro, S. Asmus, S. Beckendorf, C. Mück-Lichtenfeld and O. G. Mancheño, *J. Am. Chem. Soc.*, 2014, **136**, 13999–14002.

33 T. Ikai, *Polym. J.*, 2017, **49**, 355–362.

34 T. Ikai, S. Shimizu, S. Awata and K. Shinohara, *Macromolecules*, 2018, **51**, 2328–2334.

35 T. Ikai, K. Takayama, Y. Wada, S. Minami, C. Apiboon and K. Shinohara, *Chem. Sci.*, 2019, **10**, 4890–4895.

36 M. Nakajima, M. Saito, M. Shiro and S. Hashimoto, *J. Am. Chem. Soc.*, 1998, **120**, 6419–6420.

37 B. Bai, H.-J. Zhu and W. Pan, *Tetrahedron*, 2012, **68**, 6829–6836.